Springer

KSME

Journal of Mechanical Science and Technology 24 (2) (2010) 601~608
www.springerlink.com/content/1738-494x
DOI 10.1007/s12206-010-0106-0

# Reduced order model of three-dimensional Euler equations using proper orthogonal decomposition basis †

Sangook Jun[1], Kyung-Hyun Park[1], Hyung-Min Kang[1], Dong-Ho Lee[2,*] and Maenghyo Cho[1]

[1]*School of Mechanical and Aerospace Engineering, Seoul National University, Seoul, 151-742, Korea*
[2]*School of Mechanical and Aerospace Engineering/ Institute of Advanced Aerospace Technology, Seoul National University, Seoul, 151-742, Korea*

(Manuscript Received July 6, 2009; Revised November 17, 2009; Accepted November 23, 2009)

**Abstract**

This study seeks to validate the accuracy and the efficiency of the aerodynamic reduced order model (ROM). In doing this, snapshot data are generated from the full system analysis of a fighter wing problem. From an eigensystem analysis of these snapshots, the basis vector reproducing the behavior of the full system is obtained. The span length, sweep angle, dihedral angle, and spar and rib thickness representing the wing configuration are determined as the input variables. The constructed ROM is applied to the fighter wing problem while varying the input conditions for validation. Subsequently, a comparison of the reduced system with the full system confirmed that the aerodynamic performance is within 4% error and that the $L_2$ norms are $10^{-6}$ order of the entire flow field. Therefore, the ROM is able to capture the variation of the aerodynamic performance with respect to the input variables. Though there are structural input variables which influence the aerodynamic performance indirectly, the ROM can reproduce the flow field of the full system. Additionally, even if the ROM incurs a high computational cost to generate snapshots, it can represent the behavior of the full system efficiently once the reduced order model is constructed.

*Keywords*: Aerodynamics/structure coupling analysis; Proper orthogonal decomposition; Reduced order model; Wing-fuselage system

## 1. Introduction

Recently, numerous improvements have been made in computing systems and in computational fluid dynamics (CFD) which have enhanced the computational efficiency and accuracy in this area. However, the demand for high-fidelity simulations regarding complex flow phenomena continues to result in a substantial increase of computational time. Especially in aeroelastic problems such as flutter problems or in the design of a full-scale integrated system such as a wing-fuselage system, a CFD analysis is limited due to its high computational cost.

To enhance the computational efficiency in CFD, the reduced order model (ROM) has been implemented with CFD analysis tools [1]. The main feature of the ROM is that it increases the computational efficiency and reduces the numerous degrees of freedom (DOF) of the full system (flow variables) by performing singular value decomposition (SVD) from the solutions of Euler or Navier-Stokes problems. In other words, through proper orthogonal decomposition (POD), a small number of basis vector sets are extracted from the experimental data or the analysis results that are able to express the crucial features of the flow field. The solution to the ROM is obtained quickly in the low-dimensional space composed of these basis vector sets and is then transformed to the solution of the full system through a mapping function of the reduced system [2, 3].

As a result of this significant advantage, a considerable amount of ROM-related research has been done. Lucia extended the ROM to high-speed compressible fluid flows and applied it to a blunt body problem [2]. In his research, he developed the domain decomposition approach with an internal boundary condition to treat a region containing a moving shock wave. Kim proposed an efficient time-domain system identification and model reduction technique for linear dynamic systems (single-composite-input/eigensystem realization algorithm; SCI/ERA) which enables the effective construction of an ROM compared to previous schemes such as Pulse/ERA [4]. Beran et al. implemented a full model which couples two-dimensional Euler equations and the von Kármán equation and constructed a limit-cycle oscillation ROM [5]. However, the advantage of the ROM is not proved in three-dimensional Euler problems with unstructured grids. In addition, numerical testing is incomplete regarding predictions of

† This paper was recommended for publication in revised form by Associate Editor Do Hyung Lee

*Corresponding author. Tel.: +82 2 880 7386, Fax.: +82 2 882 7927
E-mail address: donghlee@snu.ac.kr

the aerodynamic performance with changes in structural variables such as the thickness of the rib or the spar. Hence, the need to create an ROM remains for these types of aerodynamics/structure coupling analyses.

Therefore, the objectives of this research are to construct ROMs for an aerodynamic solver and an aerodynamics/structure coupling solver and to validate their ability to predict the aerodynamic performance accurately and efficiently. To this end, snapshot data are extruded for the input variables that define the wing configuration. ROMs are constructed with the POD basis vector sets obtained from these snapshots and then are applied to fighter wing and wing-fuselage problems. Comparing the results of the reduced system with those of the full system, it will be shown that the ROM has the capability of predicting the aerodynamic performance considering several input variables, especially structural input variables such as the spar and rib thickness.

## 2. Numerical approaches

### *2.1 Aerodynamic model*

The governing equations for inviscid flow are known as Euler equations. For the conservation of mass, momentum and energy of an ideal gas, the integral form of the three-dimensional Euler equations are as follows:

$$\frac{\partial}{\partial t}\int_{\Omega} Q dV + \int_{\partial\Omega} F(Q)\cdot\vec{n} dS = 0 \tag{1}$$

The conservative variables Q and inviscid flux vectors $F(Q)\cdot\vec{n}$ are defined as Eq. (2).

$$Q = \begin{pmatrix} \rho \\ \rho u \\ \rho v \\ \rho w \\ \rho e \end{pmatrix}, \quad F(Q)\cdot\vec{n} = \begin{pmatrix} \rho V \\ \rho u V \\ \rho v V \\ \rho w V \\ \rho e V + pV \end{pmatrix} + p\begin{pmatrix} 0 \\ n_x \\ n_y \\ n_z \\ 0 \end{pmatrix} \tag{2}$$

$$where, \quad V = \vec{V}\cdot\vec{n} = un_x + vn_y + wn_z$$

In this study, inviscid fluxes at cell interfaces are computed using Roe's flux-difference-splitting scheme. The Gram-Schmidt process and QR decomposition with van Leer limiter are used for the spatial discretization. The block Gauss Seidel method is used for implicit time integration. Local time stepping and residual smoothing are applied for convergence acceleration [6-9].

Because the flow condition of the reduced order model in this research is characterized by a Mach 0.87 and an angle of attack of 2 degrees, the flow field around the ONERA M6 wing is evaluated and compared to the experimental data of Schmitt [10] in order to validate the accuracy of the developed numerical analysis code. The flow condition of the numerical analysis is set as follows: the free stream Mach number is 0.84 and the angle of attack is 3.06°. The ONERA M6 wing grid system consists of 75,313 nodes and 414,129 cells. (Fig. 1)

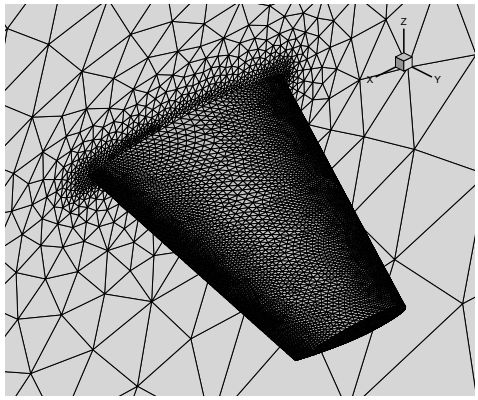


Fig. 1. Computational grids of the ONERA M6 wing.

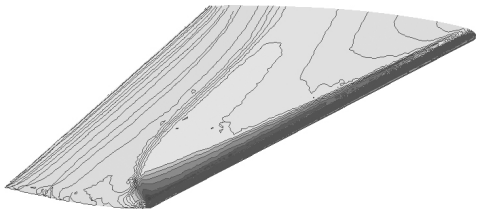

Fig. 2. Pressure distribution on the upper surface of the ONERA M6 wing.

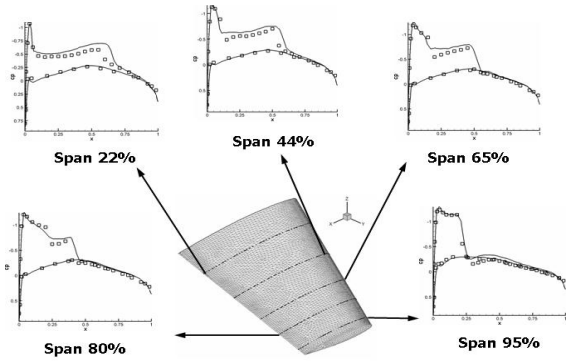


Fig. 3. Surface pressure coefficients of the ONERA M6 wing (□ : experimental results [10], ─ : computational results).

Fig. 2 shows the pressure distribution on the upper surface of the ONERA M6 wing, confirming that there is a λ shock. In addition, the distributions of the pressure coefficient at specific spanwise locations are in good agreement with the experimental data as shown in Fig. 3. Therefore, in this study, the use of the implemented code for the construction of a reduced order model is feasible.

### *2.2 Aerodynamics & structure coupling model*

The Euler solver with unstructured grids and the stress hybrid four-node shell element originally developed by Aminpour [11, 12] were used in the aerodynamics/structure coupling analysis. Additional details regarding the structural

analysis and its validation can be found in Cho and Kim [12]. Fig. 4 shows the overall procedure of the aerodynamics/structure coupling analysis. First, the pressure distribution on the surface of the wing is computed in the aerodynamic analysis, and this pressure is then transferred to each node of the structural mesh. After a structural analysis is performed with an aerodynamic load, the information of the deflected wing tip is returned to the aerodynamic analysis. Aerodynamic meshes are regenerated and the aerodynamic analysis is executed again. While transferring the aerodynamic load and the deformed wing shape, a pressure mapping algorithm [13, 14] and a displacement mapping algorithm [15, 16] using a spring analogy are used. Additional detail regarding the aerodynamics/structure coupling analysis is available in the literature [13]. In this study, the tight coupling method is used because this method improves the computational efficiency. The tight coupling method involves a transfer of the deflection of the wing shape at the intermediate stage of the aerodynamic analysis [17].

### *2.3 Reduced order model – proper orthogonal decomposition (POD)*

POD [2] is a technique used to reproduce the behavior of an overall fluid system using an orthogonal basis comprised of a small number of degrees of freedom (DOF). Because the application of POD modes excludes some of the high frequency content, the time step size can be increased for better stability using POD.

For simplicity, only one fluid variable, $\underline{w}(t)$, is considered. $\underline{w}(t)$ is spatially discretized using N nodes, including the density ($\rho$), velocity field ($u$, $v$, $w$) and energy ($e$) in the Euler equations. For this fluid variable, the full system dynamics using a nonlinear operator $R$ is depicted in Eq. (3).

$$\frac{\partial w}{\partial t} + R(\underline{w}) = 0 \tag{3}$$

POD produces a linear transformation $\Psi$ between the full system solution and the reduced order system solution. The relationship between these variables is given in Eq. (4).

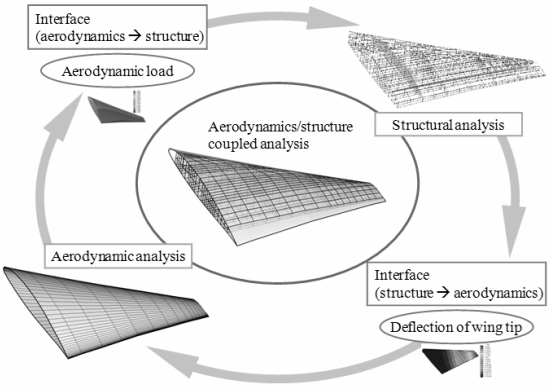


Fig. 4. Schematic of aerodynamics & structure coupling analysis.

$$\underline{w}(t) = \underline{W}_0 + \Psi \hat{\underline{w}}(t) \tag{4}$$

In this equation, $\Psi$ is not time-varying, whereas $\underline{w}(t)$ and $\hat{\underline{w}}(t)$ are functions of time $t$. The reduced order variable $\hat{\underline{w}}(t)$ represents deviations of $\underline{w}(t)$ from the base solution of $\underline{W}_0$. $\Psi$ is obtained by collecting the solution $\underline{w}(t) - \underline{W}_0$ that is observed at different time intervals from time integration of the full system or at several steady-state solutions of various flow conditions. These observations are known as snapshots and are selected as results that generally have various flow fields and that minimize linear dependency.

From the number of snapshots (length $N$) $Q$, the snapshot matrix is constructed as $N \times Q$ matrix $S$ and is decomposed via singular value decomposition. A new basis for the linear space is identified and the linear space is regenerated to approximate the original full domain and the nonlinear operator $R$. The mapping function $\Psi$ is produced as expressed by Eq. (5).

$$\begin{aligned} S^T SV &= V\Lambda \\ \Psi &= SV \end{aligned} \tag{5}$$

In this equation, the matrix $V$ is the matrix of eigenvectors of $S^TS$, and $\Lambda$ is the diagonal matrix of the eigenvalues. To eliminate redundancy in the snapshots, the columns of $V$ with very small eigenvalues are truncated and the size of the matrix of eigenvalues $\Lambda$ is adjusted. If the columns of $Q$-$M$ from $V$ are eliminated, the mapping function $\Psi$ will be an $N \times M$ matrix. This reduced order mapping is the modal representation of the flow field. The modes are the columns of $\Psi$ which are a combination of discretized spatial functions that are fixed for all time. The vector $\hat{\underline{w}}(t)$ is a time-dependent set of the coefficients representing the coordinates of $\underline{w}(t)$ projected into the truncated linear space described by the POD basis.

## 3. Results & discussions

The aerodynamic reduced order model (ROM) was applied to the wing-fuselage and the fighter wing problems for validation as summarized in Table 1.

Case 1 is the ROM of the wing-fuselage system, and Case 2 is the ROM of the wing system. The first of these performs the aerodynamic analysis with three input variables that determine

Table 1. Summary of validation cases.

| | Case 1 | Case 2 |
|---|---|---|
| Problem | wing-fuselage | wing |
| Flow condition | Mach # 0.87<br>AoA : 2 degree | Mach # 0.87<br>AoA : 2 degree |
| Input variables | span<br>sweep angle<br>dihedral angle | span<br>sweep angle<br>dihedral angle<br>spar thickness<br>rib thickness |
| Analysis | aerodynamics | aerodynamics/<br>structure |

the external shape of the wing. The second executes the aerodynamics/structure coupling analysis with five input variables, including the rib and spar thickness. The flow condition for the two cases is characterized by a Mach number of 0.87 and an angle of attack of 2 degrees.

### *3.1 Case 1 – ROM of the wing-fuselage system*

To extrude the snapshot data in Case 1, an aerodynamic analysis is performed with the unstructured grids of the wing-fuselage system as shown in Fig. 5. There are 56,348 nodes and 287,798 cells with 32,778 faces used in the boundary surfaces. For computational efficiency, only half of the geometry is considered due to the symmetry that exists in this model.

As summarized in Table 2, three input variables (span length, sweep angle, dihedral angle) were selected and eight snapshots were collected over the space of interest.

Table 2. Snapshot data of Case 1.

| | Span (m) | Sweep (deg.) | Dihedral (deg.) |
|---|---|---|---|
| snapshot 1 | 3.7760 | 32.5 | -2.5 |
| snapshot 2 | 3.7760 | 32.5 | 2.5 |
| snapshot 3 | 3.7760 | 37.5 | -2.5 |
| snapshot 4 | 3.7760 | 37.5 | 2.5 |
| snapshot 5 | 4.1956 | 37.5 | 0.0 |
| snapshot 6 | 4.6151 | 32.5 | 2.5 |
| snapshot 7 | 4.6151 | 35.0 | -2.5 |
| snapshot 8 | 4.6151 | 37.5 | 2.5 |

Table 3. Cases for validation of reduced order model.

| | Span (m) | Sweep (deg.) | Dihedral (deg.) |
|---|---|---|---|
| validation 1 | 3.7760 | 35.0 | 0.0 |
| validation 2 | 4.1956 | 32.5 | -2.5 |
| validation 3 | 4.1956 | 32.5 | 2.5 |
| validation 4 | 4.1956 | 35.0 | 2.5 |
| validation 5 | 4.6151 | 32.5 | -2.5 |
| validation 6 | 4.6151 | 32.5 | 0.0 |
| validation 7 | 4.6151 | 37.5 | -2.5 |
| validation 8 | 4.1956 | 35.0 | 0.0 |

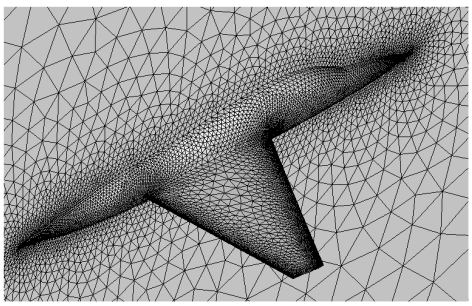

Fig. 5. Computational grids of the wing-fuselage system for Case 1.

An $S^TS$ matrix was constructed with these snapshots as mentioned in the previous section. The basis vector sets were obtained from the singular value decomposition to predict the flow field for the space in which the span length was 3.7760-4.6151 m, the sweep angle was 32.5-37.5 degrees and the dihedral angle was -2.5-2.5 degrees. The aerodynamic ROM was constructed from these vectors. To validate the constructed ROM, the results of the reduced system were compared with those of the full system for the eight conditions listed in Table 3. These are summarized in Table 4. In Table 4, the $L_2$ norm value of the last column refers to the difference in the five properties (the density, three velocity components and the total energy) of the full system compared to those of the reduced system for all of the grids. The lift-to-drag ratio, the lift coefficient and the drag coefficient were within 4.6% error, and because all $L_2$ norms are below the order of $10^{-6}$, the constructed ROM is confirmed to be in good agreement with the full system.

In Fig. 6, the pressure coefficient distribution of Validation # 5 is represented as it possesses the largest error of 4.60%. The low-pressure region around the wing tip in the reduced system is smaller than that in the full system. This difference occurs because the ROM represents a flow field with a linear combination of its basis vector sets. However, the trend of the pressure coefficient distribution of the reduced system is similar to that of the full system.

If a full system analysis is performed with a computer consisting of a Pentium D 3.0 processor with 2GB of RAM, each

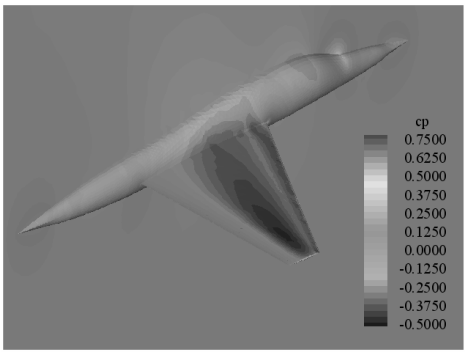


(a) Full system

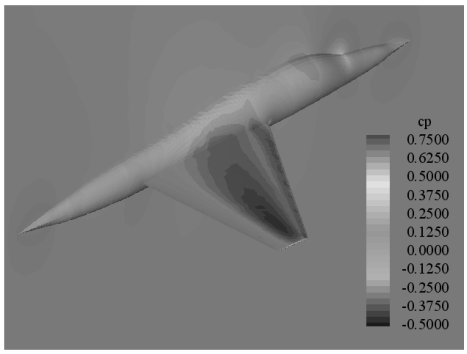


(b) Reduced system

Fig. 6. Comparison of pressure coefficient (Validation # 5).

Table 4. Comparison of aerodynamic performances (Case 1).

| | full system | | | reduced system | | | $L_2$ norm |
|---|---|---|---|---|---|---|---|
| | L/D | $C_L$ | $C_D$ | L/D | $C_L$ | $C_D$ | |
| Validation 1 | 33.4820 | 0.2385 | 0.0071 | 33.8307 (1.04%) | 0.2461 (3.17%) | 0.0073 (2.11%) | $1.35\times10^{-6}$ |
| Validation 2 | 33.2352 | 0.2522 | 0.0076 | 33.6376 (1.21%) | 0.2478 (1.74%) | 0.0074 (2.92%) | $1.95\times10^{-6}$ |
| Validation 3 | 33.1464 | 0.2572 | 0.0078 | 33.5748 (1.29%) | 0.2543 (1.11%) | 0.0076 (2.37%) | $1.49\times10^{-6}$ |
| Validation 4 | 33.8446 | 0.2572 | 0.0076 | 34.0312 (0.55%) | 0.2539 (1.30%) | 0.0075 (1.84%) | $9.44\times10^{-7}$ |
| Validation 5 | 33.7281 | 0.2677 | 0.0079 | 34.1166 (1.15%) | 0.2583 (3.50%) | 0.0076 (4.60%) | $2.46\times10^{-6}$ |
| Validation 6 | 33.6406 | 0.2701 | 0.0080 | 33.8873 (0.73%) | 0.2609 (3.38%) | 0.0077 (4.08%) | $1.93\times10^{-6}$ |
| Validation 7 | 35.3362 | 0.2646 | 0.0075 | 34.3544 (2.78%) | 0.2577 (2.60%) | 0.0075 (0.19%) | $2.24\times10^{-6}$ |
| Validation 8 | 33.8962 | 0.2549 | 0.0075 | 34.1245 (0.67%) | 0.2529 (0.79%) | 0.0074 1.46%) | $9.04\times10^{-7}$ |

Table 5. Comparison of computational time (Case 1).

| Full order analysis | Reduced order analysis |
|---|---|
| Analysis time for one case : 5732.40 sec. | Time to construct reduced order model : 176.22 sec. Time to predict a flow field : 3.31 sec. |
| Total 5732.40 sec. | Total 179.53 sec. |

case requires nearly 90 minutes, as shown in Table 5. On the other hand, in the reduced order model, constructing the basis vector requires 176 seconds and predicting the flow field requires approximately 3 seconds. Naturally, because a full system analysis is needed to generate snapshots, several hours must be reserved for a large number of snapshots. However, once the snapshots are prepared, only 3 minutes is required to predict the flow field for the range of the input variables. Therefore, the aerodynamic ROM can be used efficiently in disciplines which require numerous aerodynamic results, e.g., aeroelastics, design optimization and others.

### *3.2 Case 2 – ROM of the wing system*

The aerodynamics/structure coupling analysis is completed with the grids of the fighter wing system as shown in Fig. 7. There are 48,652 nodes and 244,311 cells for the aerodynamic grids, and 678 nodes and 796 elements are used in the structural meshes.

In Case 2, to confirm that the ROM can capture the effect of the structural variables on the aerodynamic performance, the spar and rib thicknesses were added to the input variables used in Case 1. If the aerodynamic analysis is performed alone, the spar and rib thickness cannot affect the aerodynamic performance. However, in the aerodynamics/structure coupling analysis, because the deflection of the wing tip is caused by the

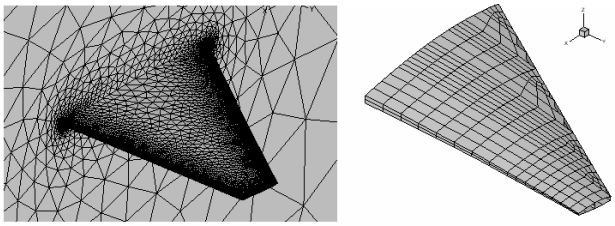

(a) Aerodynamic grids (b) Structural grids

Fig. 7. Computational grids of the fighter wing system for Case 2.

aerodynamic load, the aerodynamic performance differs from that in the single aerodynamic analysis. Additionally, a thicker spar and rib for an identical aerodynamic load leads to a smaller deflection of the wing tip. Therefore, the ROM in Case 2 was constructed from snapshots of the aerodynamics/structure coupling analysis and then compared to the full system. The flow condition is characterized by a Mach number of 0.87 and an angle of attack of 2 degrees, as in Case 1. For the structural analysis, it was assumed that Al2024-T6 comprised the material property of the spar and the rib. The snapshot data of Case 2 is summarized in Table 6.

The snapshot matrix was generated and the ROM of the aerodynamics/structure coupling analysis was then constructed. This reduced system was validated for the cases given in Table 7, and the results are shown in Table 8. In Table 7, Validation # 3 / # 4 and Validation # 5 / # 6 are cases in which the spar and rib thickness were varied and other variables were fixed. The variation of the spar or rib thickness does not have a significant effect on the aerodynamic performance compared to the effects of other input variables. However, simultaneous variation of the spar and rib thickness can have a nontrivial influence on the aerodynamic performance. Therefore, these two structural input variables were changed simultaneously to confirm the effect on the aerodynamic performance.

Table 6. Snapshots of Case 2.

| | Span (m) | Sweep (deg.) | Dihedral (deg.) | Spar thickness (cm) | Rib thickness (cm) |
|---|---|---|---|---|---|
| Snapshot 1 | 3.7760 | 32.5 | -2.5 | 0.2 | 0.5 |
| Snapshot 2 | 3.7760 | 32.5 | -2.5 | 3.0 | 0.1 |
| Snapshot 3 | 4.6151 | 35.0 | -2.5 | 0.2 | 0.5 |
| Snapshot 4 | 3.7760 | 37.5 | -2.5 | 1.6 | 0.5 |
| Snapshot 5 | 4.1956 | 37.5 | -2.5 | 0.2 | 0.5 |
| Snapshot 6 | 4.6151 | 37.5 | -2.5 | 3.0 | 0.1 |
| Snapshot 7 | 4.6151 | 32.5 | 0.0 | 3.0 | 0.3 |
| Snapshot 8 | 3.7760 | 37.5 | 0.0 | 3.0 | 0.1 |
| Snapshot 9 | 3.7760 | 32.5 | 2.5 | 0.2 | 0.1 |
| Snapshot 10 | 3.7760 | 32.5 | 2.5 | 3.0 | 0.1 |
| Snapshot 11 | 3.7760 | 32.5 | 2.5 | 3.0 | 0.5 |
| Snapshot 12 | 4.6151 | 32.5 | 2.5 | 0.2 | 0.3 |
| Snapshot 13 | 4.6151 | 32.5 | 2.5 | 3.0 | 0.1 |
| Snapshot 14 | 3.7760 | 37.5 | 2.5 | 1.6 | 0.1 |
| Snapshot 15 | 4.1956 | 37.5 | 2.5 | 3.0 | 0.3 |

Table 7. Cases for validation of reduced order model.

| | Span (m) | Sweep (deg.) | Dihedral (deg.) | Spar thickness (cm) | Rib thickness (cm) |
|---|---|---|---|---|---|
| Validation 1 | 4.1956 | 35.0 | -2.5 | 3.0 | 0.1 |
| Validation 2 | 3.7760 | 37.5 | -2.5 | 3.0 | 0.5 |
| Validation 3 | 4.1956 | 32.5 | 0.0 | 0.2 | 0.1 |
| Validation 4 | 4.1956 | 32.5 | 0.0 | 1.6 | 0.5 |
| Validation 5 | 3.7760 | 35.0 | 0.0 | 0.2 | 0.3 |
| Validation 6 | 3.7760 | 35.0 | 0.0 | 3.0 | 0.5 |
| Validation 7 | 3.7760 | 37.5 | 2.5 | 0.2 | 0.5 |
| Validation 8 | 4.1956 | 35.0 | 0.0 | 1.6 | 0.3 |

In Validation # 3-# 6 of Table 8, the error of the ROM is within 3.5% due to the variation of the structural variables. This is lower than the error resulting from the variation of the other input variables (4.36% in Validation # 2). In other words, the ROM of the aerodynamics/structure coupling analysis is capable of predicting the aerodynamic performance if the effect of the structural variables is included in the snapshot data obtained from the full system analysis.

The pressure coefficient distribution of Validation # 2 has the largest error, at 4.36%, as shown in Fig. 8. It can be confirmed that the $C_P$ contour of the reduced system is very similar to that of the full system.

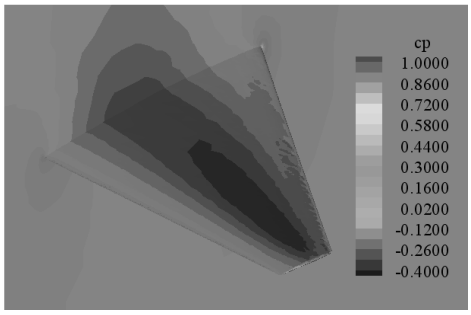


(a) Full system

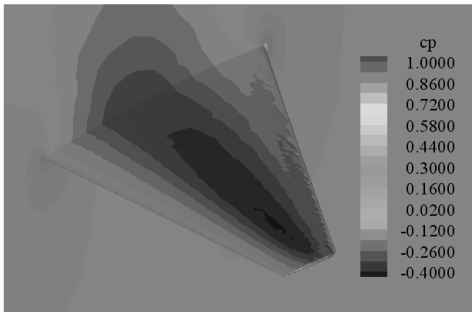


(b) Reduced system

Fig. 8. Comparison of pressure coefficients (Validation # 2).

Table 8. Comparison of aerodynamic performances (Case 2).

| | Full system | | | | Reduced system | | | | $L_2$ norm |
|---|---|---|---|---|---|---|---|---|---|
| | L/D | $C_L$ | $C_D$ | Tip deflection (cm) | L/D | $C_L$ | $C_D$ | Tip deflection (cm) | |
| Validation # 1 | 23.7559 | 0.2158 | 0.0091 | 1.8995 | 23.3908 (1.54%) | 0.2135 (1.05%) | 0.0091 (0.49%) | 1.8788 (1.09%) | $9.11 \times 10^{-7}$ |
| Validation # 2 | 23.6289 | 0.2016 | 0.0085 | 1.2152 | 23.4461 (0.77%) | 0.2088 (3.55%) | 0.0089 (4.36%) | 1.2480 (2.69%) | $1.47 \times 10^{-6}$ |
| Validation # 3 | 22.9028 | 0.2184 | 0.0095 | 1.9275 | 22.9783 (0.33%) | 0.2142 (1.91%) | 0.0093 (2.23%) | 1.9033 (1.26%) | $1.20 \times 10^{-6}$ |
| Validation # 4 | 22.9167 | 0.2186 | 0.0095 | 1.7715 | 23.1287 (0.92%) | 0.2146 (1.79%) | 0.0093 (2.69%) | 1.7531 (1.04%) | $1.27 \times 10^{-6}$ |
| Validation # 5 | 22.6655 | 0.2038 | 0.0090 | 1.2253 | 23.0847 (1.85%) | 0.2109 (3.49%) | 0.0091 (1.61%) | 1.2728 (3.88%) | $1.03 \times 10^{-6}$ |
| Validation # 6 | 22.6886 | 0.2040 | 0.0090 | 1.0695 | 23.0458 (1.57%) | 0.2108 (3.33%) | 0.0091 (1.73%) | 1.1096 (3.74%) | $9.96 \times 10^{-7}$ |
| Validation # 7 | 23.2121 | 0.2058 | 0.0089 | 1.3655 | 23.2873 (0.32%) | 0.2120 (3.01%) | 0.0091 (2.68%) | 1.4202 (4.00%) | $1.99 \times 10^{-6}$ |
| Validation # 8 | 23.5861 | 0.2182 | 0.0093 | 1.9040 | 23.3307 (1.08%) | 0.2146 (1.63%) | 0.0092 (0.56%) | 1.8865 (0.92%) | $5.91 \times 10^{-7}$ |

Table 9. Comparison of computational time (Case 2).

| Full order analysis | Reduced order analysis |
|---|---|
| Analysis time for one case : 7069.50 sec. | Time to construct reduced order model : 289.33 sec. Time to predict a flow field : 2.92 sec. |
| Total 7069.50 sec. | Total 292.25 sec. |

With the same environment and computer resources used in Case 1, the computational time of the full system analysis is nearly 2 hours per case, as shown in Table 9. However, in the ROM, constructing the basis vector sets from the eigensystem analysis requires 290 seconds and predicting the flow field takes nearly 3 seconds. The amount of snapshot data in Case 2 is twice that that in Case 1; hence, the cost of obtaining the basis vector sets doubles as well. As mentioned earlier, because the amount of snapshot data indicates the number of the degrees of freedom that adequately reproduces the behavior of the full system, a greater number of input variables implies that additional snapshots are required. However, even if the number of snapshots is increased, a full system analysis is no longer required for the space of interest. Therefore, the use of the ROM is efficient in disciplines requiring a great deal of aerodynamic analysis.

## 4. Conclusions

In this study, reduced order models of a three-dimensional Euler code with unstructured grids and an aerodynamics/structure coupling analysis code are constructed. The snapshot data are generated for the input variables which represent the fighter wing configuration. The basis vector sets which reproduce the behavior of the full system are obtained through an eigensystem analysis. The constructed reduced order models are compared and validated with the results of the full system analysis. These results lead to several conclusions.

First, it was confirmed that the reduced order model constructed with several input variables is capable of predicting the aerodynamic performance. In Cases 1 and 2, the lift-to-drag ratio, the lift coefficient and the drag coefficient of the reduced order models show discrepancy within 4.6% from those of the full system. Additionally, the $L_2$ norm value for all of the grids is on the order of $10^{-6}$; hence, the reduced order model thoroughly reproduces the flow field for the space and condition of interest.

Second, the reduced order model can capture the influence of the structural input variables on the aerodynamic performance. Because the aerodynamic load results in the deflection of the wing tip, the spar and rib thickness influence the aerodynamic performance indirectly. Therefore, if the effect of any structural deflection is included in the snapshot data, a reduced order model constructed with these snapshots can reflect the variation of the aerodynamic performance with respect to the structural deflection of the wing. Additionally, compared to the other input variables, the variation of the structural input variables has little effect on the accuracy of the reduced order model.

Finally, though the reduced order model incurs a high computational cost when generating snapshots, predictions of the flow field in conditions of interest only require several seconds once the reduced order model is constructed. This demonstrates that the reduced order model would be efficient in disciplines that require a great deal of aerodynamic analysis, such as aeroelastics or design optimization.

## Acknowledgment

We appreciate the support of the Defense Acquisition Program Administration and Agency for Defense Development for this study to be completed under the contract UD070041AD, the Institute of Advanced Aerospace Technology at Seoul National University and the second stage of the Brain Korea 21 Project in 2009.

## Nomenclature

| | | |
|---|---|---|
| $AoA$ | : | Angle of attack |
| $C_D$ | : | Drag coefficient |
| $C_L$ | : | Lift coefficient |
| $C_P$ | : | Pressure coefficient |
| $e$ | : | Total internal energy |
| $F$ | : | Inviscid flux vectors |
| $L/D$ | : | Lift to drag ratio |
| $N$ | : | The number of nodes in full system |
| $\vec{n}$ | : | Normal vector on control surface |
| $p$ | : | Pressure |
| $Q$ | : | Conservative variables or the number of snapshots |
| $R$ | : | Residual or nonlinear operation |
| $S$ | : | Control surface or snapshot matrix |
| $t$ | : | Time |
| $u$ | : | Velocity components in the x-direction |
| $V$ | : | Control volume or matrix of eigenvectors of $S^TS$ |
| $v$ | : | Velocity components in the y-direction |
| $w$ | : | Velocity components in the z-direction |
| $\underline{w}$ | : | Full system solution |
| $\underline{W}_0$ | : | Base solution |
| $\underline{\hat{w}}$ | : | Reduced system solution |
| $\Lambda$ | : | Diagonal matrix of eigenvalues of STS |
| $\rho$ | : | Density |
| $\Psi$ | : | Linear transformation |
| $\Omega$ | : | Cell volume |
| $\partial\Omega$ | : | Boundary of domain Ω |
| $W$ | : | Effective work |

## References

[1] D. J. Lucia, P. S. Beran and W. A. Silva, Reduced-order modeling: new approaches for computational physics, *Aerospace Science*, 40 (2004) 51-117.

[2] D. J. Lucia, Reduced Order Modelling for High Speed Flows

With Moving Shocks, Ph. D Thesis, Air Force Institute of Technology, School of Engineering and Management, (2001).

[3] P. Holmes, J. L. Lumley and G. Berkooz, Turbulence, *Coherent Structures, Dynamical Systems and Symmetry*, *Cambridge University Press*, Cambridge, UK, (1996).

[4] Taehyoun Kim, Efficient Reduced-Order System Identification for Linear Systems with Multiple Inputs, *AIAA journal*, 43 (7) (2005) 1455-1464.

[5] P. S. Beran, D. J. Lucia and C. L. Pettit, Reduced-Order Modelling of Limit-Cycle Oscillation for Aeroelastic Systems, *Journal of Fluids and Structures*, 19 (2004) 575-590.

[6] G. A. Ashford, An Unstructured Grid Generation and Adaptive Solution Technique for High-Reynolds-Number Compressible Flows, Ph. D thesis, University of Michigan, (1996).

[7] D. L. Whitaker, Two-dimensional Euler Computations on a Triangular Mesh Using an Upwind, Finite-Volume Scheme, Ph. D thesis, Virginia Polytechnic Institute and State University, (1988).

[8] W. K. Anderson and D. L. Bonhaus, An Implicit Upwind Algorithm for Computing Turbulent Flows on Unstructured Grids, *Computer Fluids*, 23 (1) (1994) 1-21.

[9] V. Venkatakrishnan, Convergence to Steady Solutions of the Euler Equations on Unstructured Grids with Limiters, *Journal of computational physics*, 118 (1995) 120-130.

[10] V. Schmitt and F. Charpin, Pressure Distributions on the ONERA-M6-Wing at Transonic Mach Numbers, Experimental Data Base for Computer Program Assessment. Report of the Fluid Dynamics Panel Working Group 04, AGARD AR 138, May 1979.

[11] M. A. Aminpour, An assumed stress hybrid 4 node shell element with drilling degrees of freedom, *International Journal for Numerical Methods in Engineering*, 33 (1992) 11-38.

[12] Maenghyo Cho and Hyungi Kim, A refined semi-analytic design sensitivity based the mode decomposition and Neumann series, *International Journal for Numerical Methods in Engineering*, 62 (2005) 19-49.

[13] D. S Choi, J. O. Jun, B. K. Kim, S. H. Park, M. H. Cho, D. H. Lee, K. T. Lee and S. M. Jun, Static Aeroelastic Analysis for Aircraft Wings using CFD/CST Coupling Methodology, *Journal of the Korea Society for Aeronautical and Space Sciences*, 35 (4) (2007) 287-294.

[14] M. K. Bhardwaj, A CFD/CSD Interaction Methodology for Aircraft Wings, Ph.D. thesis, Department of Aerospace Engineering, The Virginia State University at Blacksburg, Virginia, (1997).

[15] J. T. Batina, Unsteady Euler Airfoil Solutions Using Unstructured Dynamic Meshes, *AIAA Journal*, 28 (8) (1990) 1381~1388.

[16] B. K. Kim, S. O. Jun, Y. H. Jeon, J. H. Kim and D. H. Lee, Efficiency of Dynamic Mesh in Static Aeroelastic Analysis and Design Optimization Problem, *Journal of the Korea Society for Aeronautical and Space Sciences*, 35 (2) (2007) 87-93.

[17] Y. S. Kim, J. Kim, Y. H. Jeon, J. S. Bang, D. H. Lee, Y. H. Kim and C. Park, Multidisciplinary Aerodynamic-Structural Design Optimization of Supersonic Fighter Wing Using Response Surface Methodology, *40th AIAA Aerospace Sciences Meeting and Exhibit*, Reno, Nevada, USA, (2002) AIAA-2002-0322.

**Sangook Jun** is a Ph.D candidate, in the integrated MA/Ph.D Course at Seoul National University. His B.S degree is from Seoul National University. The research topic of interest is a robust design optimization and a reduced order model.

**Dongho Lee** is a professor at Seoul National University. A member of The National Academy of Engineering of Korea, he is also the director of Institute of Advanced Aerospace Technology, Seoul National University. He is interested in Computational Fluid Dynamics, wind tunnel test and Multidisciplinary Design Optimization for large and complex systems (e.g. aircraft, helicopter, high speed train, compressor and wind turbine).